Efficient fluorescence image normalization for time lapse movies

Michael Schwarzfischer[1*], Carsten Marr[1*], Jan Krumsiek[1], Philipp S. Hoppe[2], Timm Schroeder[2],
Fabian J. Theis[1,3]

[1]Institute of Bioinformatics and Systems Biology, Helmholtz Zentrum München, Neuherberg, Germany
[2]Research Unit Stem Cell Dynamics, Helmholtz Zentrum München, Neuherberg, Germany
[3]Department of Mathematics, Technische Universität München, Garching, Germany

Abstract— In the last few years, single-cell time-lapse fluorescence microscopy has emerged as a key technology in the toolbox of experimental life science. Imaging fluorescently tagged proteins allows to combine past and future information of cellular progeny with time resolved protein dynamics. Whenever quantitative data on the intensity of the fluorescence signal is required, a careful image processing pipeline has to be applied to account for uneven illumination, background signal, varying illumination strength or photobleaching. Previous approaches commonly used an additional calibration step to infer such image characteristics by imaging fluorescent dilutions like fluorescein.

Here, we describe a method to infer a time-dependent background signal and the image gain without the use of additional fluorescent substances – instead, we use the information contained in the bleaching background of the fluorescence time-lapse movie itself. First, we tile the full image into small sub-images and determine background tiles by clustering the statistical moments of the individual intensity distributions. For each image, we interpolate the full background from the identified tiles and thus reconstitute the time-dependent background image. Second, we estimate the time-independent image gain from the background tiles of all pixels and all time points. We are thus able to correct for a bleaching background and an uneven illumination of the experimental setup. We show the applicability of our method by comparing the intensities of fluorescent beads derived from time-lapse microscopy with intensities inferred from FACS analysis.

In summary, our normalization method accurately corrects for fluorescence image issues and decreases the necessary experimental work.

I. INTRODUCTION

In recent years, single-cell time-lapse fluorescence microscopy has emerged as a key technology in the toolbox of biological research [1], [2], [3]. It allows to combine the information of cellular progenies with quantitative protein expression and has been used to address a wide spectrum of biological questions, from cell-to-cell variability [4] over drug response [5] to cell fate prediction [6] and cell cycle analysis [7]. The general experimental approach is to (i) tag the gene of interest with a fluorescent protein, (ii) culture the genetically modified cells, (iii) excite the culture with light of the respective wavelength and take microscopy pictures of the emitted fluorescent light. Whenever quantitative results on the intensity of the fluorescent signal are required, a careful image processing pipeline has to be applied to the microscopy images [8]. Combined with cell tracking and image segmentation, this
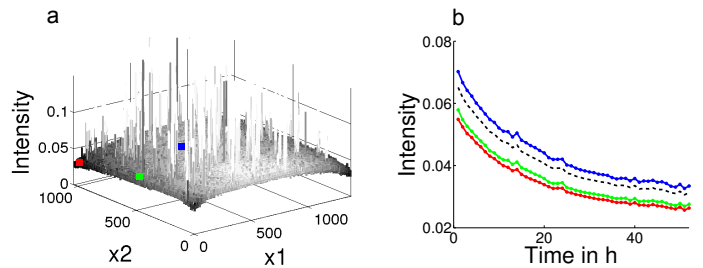
Fig. 1. Properties of time-lapse fluorescence images. (a) A typical fluorescence image with space coordinates (x_1, x_2) and fluorescence intensity plotted on the z-axis where peaks represent cellular signal. In long-term time-lapse microscopy, one has to deal with the following issues: (i) An inhomogeneous illumination due to the light source and camera lens, (ii) a non-zero background signal due to autofluorescence of the medium, and (iii) the effect of photo-bleaching (b). During an experiment the setup is sequentially illuminated with light. This leads to a bleaching effect in the medium where cells are cultured in and decreases the image intensity. The black dashed line represents the mean image intensity while the colored lines correspond to the colored dots in (a) (red: pixel in the upper left corner, green: pixel in the middle left, blue: pixel in the image center).

data contains a wealth of information of cellular behavior and protein dynamics [9].

Here, we focus on the normalization of microscopy images and propose an efficient and parsimonious technique to estimate (i) the time-dependent background signal from the medium where cells are cultured in and (ii) the time-independent gain from the optical apparatus. We infer these components from time-lapse microscopy data alone without the need for additional substances like fluorescein.

II. METHODS

A. Definitions

A raw fluorescence image $I(x, t)$ at time point t with space coordinates $x = (x_1, x_2)$ (see Fig. 1) can be decomposed into the following elements:

- a cellular signal $s(x, t)$, which changes over time.
- a homogeneous background signal $b(t)$ (e.g. autofluorescence of the culture medium), that decreases over time due to photo-bleaching.
- a coordinate-specific illumination function called *gain* $g(x)$ originating from the uneven illumination or the light source and the lens. The gain is defined as signal intensity per fluorescent molecule, which is assumed to scale linearly.
- a camera offset $o(x)$, which is constant over time.

Additional technical noise appears in equal measure at every position and time point. Since our normalization method uses robust fitting methods noise only has a marginal influence and is not discussed in the procedure presented here. Other means to infer the nature and intensity of the noise have to be applied separately.

We summarize all contributions in the following equation:

$$I(x,t) = s(x,t) \cdot g(x) + b(t) \cdot g(x) + o(x). \qquad (1)$$

By rearranging the formula we get the cellular signal by

$$s(x,t) = \frac{I(x,t) - b(t) \cdot g(x) - o(x)}{g(x)}. \qquad (2)$$

All contributions on the right hand side of equation (2) are derived with the following approach.

B. Time-dependent background estimation

We estimate the illuminated background signal including the offset, denoted as $B(x,t) = b(t) \cdot g(x) + o(x)$. By estimating $B(x,t)$ on each image separately we account for bleaching of the medium. First, our method divides the image $I(x,t)$ into small overlapping sub-images, called *tiles* (see Fig. 2). The distribution of intensities from tiles with cellular signal considerably differs from tiles without cellular signal and can be distinguished by the moments of the distribution. The appropriate selection of moments depends on the properties of the background image: for flat images, the first two moments (mean and variance) provide the most powerful means to discriminate background from cell signal, for more complicated illumination shapes with varying gradients (as shown in Fig. 2), additional higher moments will be more appropriate.

For the following steps, we represent each individual tile as a point in the multi-dimensional space of distribution moments. The datapoints of distributions of background tiles have almost equal features and will accumulate in a small dense volume. Therefore, we use a density-based clustering approach, called DBSCAN [10], which returns two clusters (see Fig. 2): One very dense cluster referring to background tiles, and a dispersed cluster from tiles containing cellular signal.

The median of each tile from the first cluster is used to reconstruct an initial background grid. Finally, a two dimensional natural neighbor inter- and extrapolation is applied, which results in an estimation of $B(x,t)$. This procedure is applied to every image independently.

C. Fitting the time-independent gain

The bleaching of each pixel is position-dependent due to the uneven illumination of the experimental setup. A pixel in the center will experience a high irradiation and therefore bleach at a faster rate (Fig. 3b). Plotting the absolute background pixel intensity against the mean background intensity for every time point reveals a linear correlation (see Fig. 3c). Every pixel behaves linearly with respect to the overall mean intensity but with different slopes. A linear regression for every pixel x yields the slope, which represents the relative gain $g'(x) = c \cdot g(x)$ (see Fig. 3d) while the ordinate-intercept

represents the offset $o(x)$. The relative gain $g'(x)$ defined as intensity per mean background signal represents the real gain $g(x)$ multiplied by a factor c. Since we correlate every pixel with the mean background intensity instead of known fluorescent molecule concentrations we can only determine this relative gain. The factor c cannot be further determined without additional experiments. However, since it is a constant factor, it does not alter the signal fold changes within the fluorescence images. It is also independent of time t and space x. To determine the factor c and finally infer protein abundances, a further calibration step must be applied. This can be done experimentally by comparing known concentrations in normalized time-lapse images or computationally with additional tracking methods as described in [11].

D. Final correction

The final relative cellular signal can be derived by

$$s'(x,t) = \frac{I(x,t) - B(x,t)}{g'(x)}, \qquad (3)$$

with

$$s'(x,t) = s(x,t) \cdot c^{-1}, \qquad (4)$$

illustrated in Fig. 4. After this normalization step all cellular signals are on a comparable intensity level. Ratios of the relative cellular signal are identical to ratios of real cell signal.

III. APPLICATION

We applied our method to a time-lapse microscopy experiment of fluorescent beads, which are commonly used for calibration in flow cytometry. Here, we used unbleached and bleached beads as a representative for two different intensities of fluorophores in a cell matrix. The bleaching itself is of no importance to our test. Thus, we were able to validate our normalization method in a maximally clean and controllable setup and compare it to the published normalization method of [12], which relies on additional imaging of a fluorescein solution and a background image.

FITC-Beads (Becton Dickinson, Heidelberg, Germany) were quantified and sorted by flow cytometry on a FACSAriaI (Becton Dickinson, Heidelberg, Germany). We included only single-bead events according to the FSC/SSC Plot and further gated the beads for high FITC fluorescence. Beads were thereby quantified and subsequently sorted. Furthermore, they were washed and plated at a density of 2700 per 0.6 cm^2 on a μ-slide VI$_{0.4}$ (IBIDI, Martinsried, Germany) in StemSpan Serum-Free Expansion Medium (StemCell Technologies, Vancouver, Canada). In different compartments StemSpan Serum-Free Expansion Medium or a 100nM fluorescein-solution in PBS (Invitrogen, Karlsruhe, Germany) were plated. Tiff-Images were acquired on a CellObserver system (Zeiss, Hallbergmoos, Germany) with a 10x Fluar objective (Zeiss) and an AxioCamHRm camera (Zeiss) at 1388x1040 pixel resolution over 17 hours at a 5 min interval with Zeiss Software AxioVision 4.7 (as described in [13]). A mercury lamp (HBO 103W/2, Osram, Augsburg, Germany) was used for fluorescence illumination at an exposure time of 500 ms with a 46 HE Filter (Zeiss). Afterwards, the FITC-Beads were
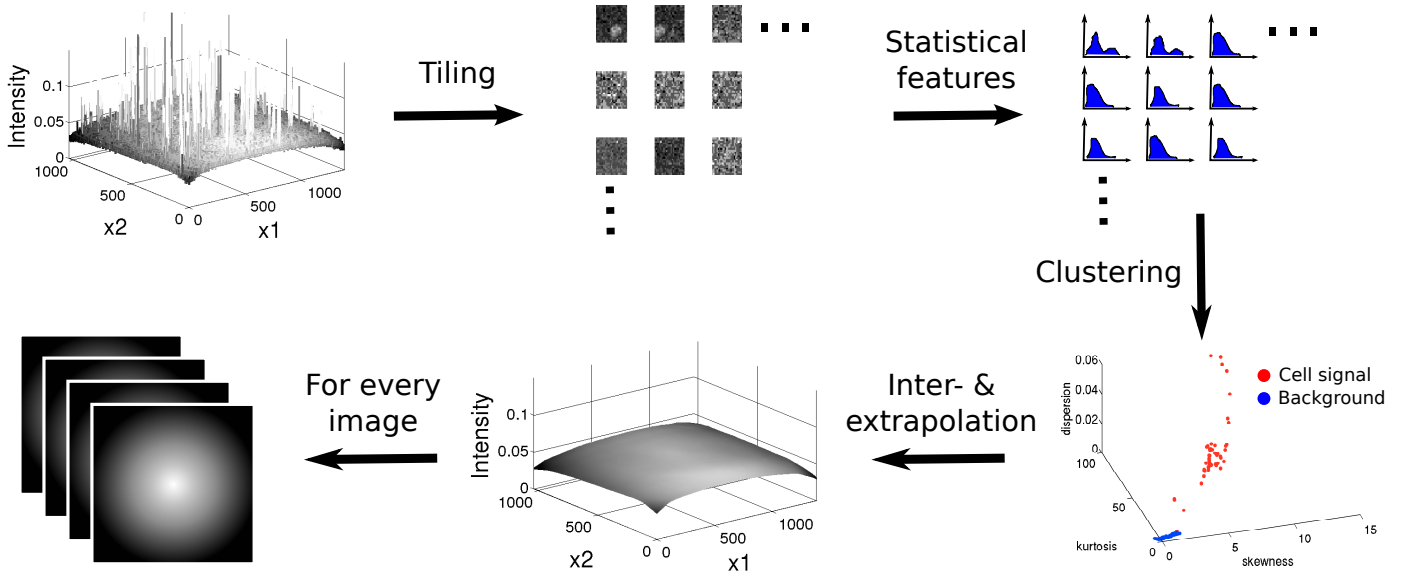
Fig. 2. Time-dependent background estimation $B(x,t)$. Each fluorescence image $I(x,t)$ is tiled into small overlapping sub-images. For each tile, the moments of the intensity distribution are calculated. A density-based clustering on the moments of the distributions splits the tiles into two clusters. The tiles containing only background are kept and their median intensity is used to construct a grid which serves as a basis for a two dimensional inter- and extrapolation to estimate the full background $B(x,t)$ of the image. This procedure is applied to every fluorescence image of the time-lapse movie.
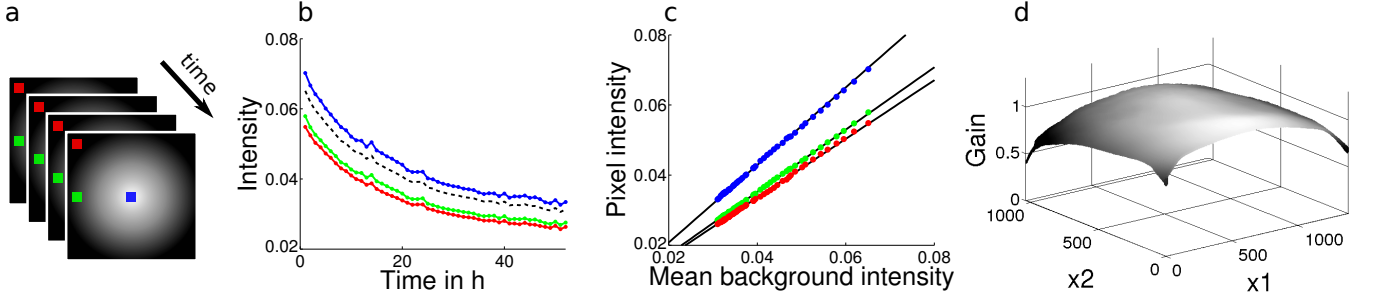

Fig. 3. Fitting the time-independent gain $g(x)$. (a) Monitoring each pixel as well as the mean in every background image $B(x,t)$ over time shows (b) the bleaching behavior of the medium. For demonstration we picked three pixels from the upper left corner (red), the left edge (green) and the center of the image (blue). The black dashed line indicates the mean background intensity. (c) A scatter plot of the mean vs. each pixel intensity reveals a linear dependence. From the ordinate intercept and the slope of the linear regression, we infer the offset $o(x)$ and the relative gain $g'(x)$ (d).
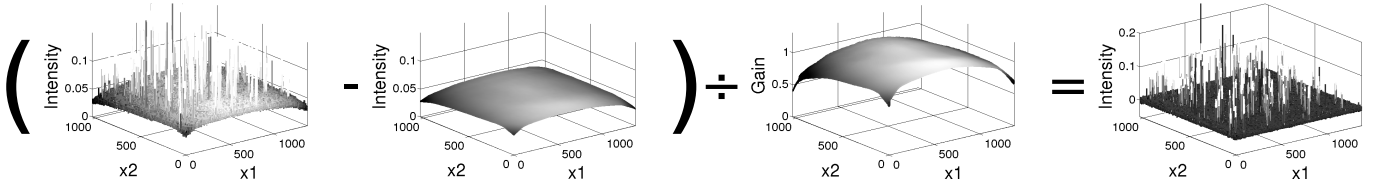

Fig. 4. Final correction $(I(x,t) - B(x,t)) \div g'(x) = s'(x,t)$. The illuminated background and the offset, $B(x,t)$, derived by the tiling method described in Fig. 2 are subtracted from the fluorescence image. The resulting image is then divided by the time-independent gain $g'(x)$, calculated from the linear regression as shown in Fig. 3. The final image contains normalized cell signal and a homogeneous background around 0.

harvested, washed and reanalyzed on a FACSAriaI using the exact same FSC/SSC gates as before.

For segmentation, we used the published tool ilastik [14] to detect bead outlines on the brightfield images, resulting in binary images. The same bead detections were used throughout all following quantifications with different normalization methods.

For our method, we used tiles of 30x30 pixels overlapping by 15 pixel and clustered on skewness, kurtosis and the fano factor (i.e. the normalized variance). For DBSCAN we set minimal number of objects considered as a cluster to 4 (number of dimensions+1) and used an adhoc value for the neighborhood radius. Following the protocol described in [12], we subtracted the background from the original image and divided it by the background-subtracted fluorescein images.

To test the applicability of this approach, we compared the intensity fold change between unbleached (at the start of the movie) and bleached (at the end of the movie) beads
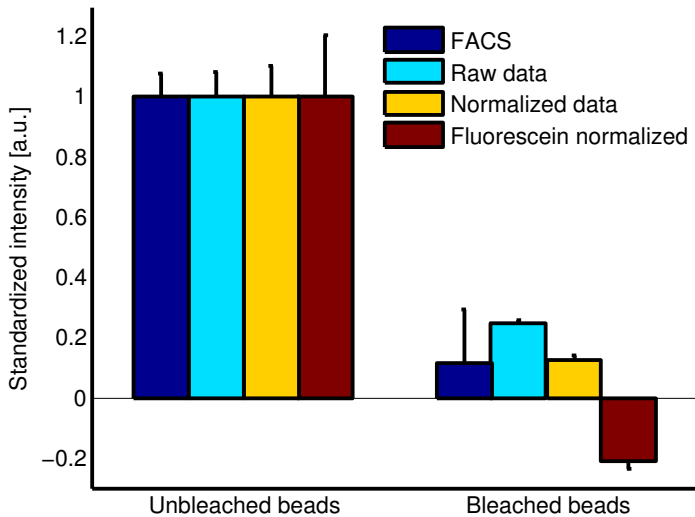
Fig. 5. Application of the method. We compare the intensity fold change between unbleached and bleached beads derived from FACS analysis and time-lapse microscopy imaging. Our normalization method (yellow) yields ratios comparable to the FACS data (blue). Additionally, the null hypothesis of equal distributions cannot be rejected by a Wilcoxon rank-sum test (p-value = 0.5531). The raw data (cyan) and the fluorescein normalized data following [12] deviate substantially (p-value of Wilcoxon rank-sum test $< 4 \cdot 10^{-8}$).

with FACS analysis and time-lapse fluorescence microscopy imaging (see Fig. 5). From FACS analysis, we inferred a 8.5 fold change between unbleached and bleached beads. This is in accordance with a 8.0 fold change, derived with our normalization method. In contrast, the raw, unnormalized data yields a fold change of 4.0, while the fluorescein normalized method described in [12] yields negative intensity values for the bleached beads (see Fig. 5).

IV. DISCUSSION

Our approach can be well compared to already published methods. The simplest thing to solely estimate the background in real data images is to take the original image and apply a 2D median filtering step with a large window size [15]. This method is a quick and easy way as long as there are no colony forming cells and the background does not have a complex illumination pattern. Moreover, it is only appropriate for images where the median of a window always corresponds to the background. A more sophisticated way of classifying intensities has been described in [16]. The authors iteratively fit a two dimensional cubic spline surface to a grid which is based on estimated background pixels. With this fit they are able to redefine the first poor estimation of pixels corresponding to background and achieve an approximation for the true background after the algorithm reaches the convergence criteria. We used the MATLAB code provided on the author's homepage (http://www.cb.uu.se/~joakim/software/) to compare it with our method. It turned out that the difference for both methods is minute regarding accuracy as well as computational performance.

Previous approaches to estimate both background and gain commonly used a calibration step to infer the space-dependent gain by imaging fluorescent dilutions like fluorescein [12]. The background or camera offset was determined by imaging

empty bins or non-fluorescent dilutions. These images were taken at different spots of the experiment and did thus not reflect the exact illumination and background at positions where the actual cell images were taken. To countervail this spatial inconsistency, it is also possible to directly include fluorescein in the cell culture and capture the illumination image in a different wavelength than the signal of interest. However, the gain detection is then flawed by cells and other contaminants in the fluid which will lead to deviations from the exact illumination pattern. Our approach uses the bleaching medium and does not rely on additional dilutions. First, we computationally estimate the time-dependent illuminated background from each cell image itself. The gain is calculated by a linear regression for each pixel against the estimated mean background intensities. This is similar to the approach described in [17], where different dilutions of GFP are used to infer the pixel gain. In this respect, the different levels of bleached medium resemble different fluorescein or GFP concentrations. Second, we have no need for further chemicals like fluorescein in the cell culture which reduces the experimental work.

Since the availability of background tiles can indeed become crucial for our method we tested the performance of our tiling method by randomly adding bright spots of 10x10 pixel, representing cellular signal within a perfect background. For each iteration we added one hundred of these spots, estimated the background with our method using 30x30 pixel tiles and calculated the root mean square difference. It turned out that our method is applicable for up to 1500 bright spots, which means that about 13% of the image is full of cells. After setting the tile size to 20x20 pixel we could still get accurate background estimations for higher cell densities. We require about 10% of all possible grid points to get an accurate background estimation. However, this threshold also depends on the performance of the used inter- and extrapolation step. Especially the extrapolation step can introduce crucial deviations from the real background.

Concerning computational needs, a two core processor, each 2.80GHz, takes about 15 seconds per single image background estimation and about one hour per gain calculation with MAT-LAB written software. If computational power is a limiting factor we propose a more parsimonious version of the method: It would suffice to apply the computationally expensive linear regression only to datapoints of the initial background grid instead of all points including interpolated pixel. After that, the inter- and extrapolation is used for the sparse gain-grid.

As a future improvement other density based cluster algorithms such as OPTICS which are parameter free can be incorporated. The choice of features for clustering (i.e. the moments of the tile distributions) still remains to the user and has to be done carefully depending on the image characteristics.

V. CONCLUSION

Fluorescence images have general issues like uneven illumination or a background signal which can also vary over time. To achieve a normalized cellular signal one has to estimate

the background level and determine the gain and camera offset. Typically, autofluorescence in the medium culture is regarded as a disturbing element in image processing. Here, we presented a method which exploits this effect to estimate the autofluorescent background, gain, and offset.

With fluorescent beads as a representative for cellular signal, we here validated our normalization method against an accurate FACS analysis. We showed that correct fold changes are only preserved if an accurate normalization method is applied. In summary, we provide a powerful method to normalize long-term time-lapse fluorescence microscopy movies. This is crucial for obtaining accurate protein expression patterns to address quantitative aspects of differentiation, cellular response, or biomolecular mechanisms in the future.

REFERENCES

[1] Dale Muzzey and Alexander van Oudenaarden, "Quantitative time-lapse fluorescence microscopy in single cells.," *Annu Rev Cell Dev Biol*, vol. 25, pp. 301–327, 2009.

[2] Michael A Rieger and Timm Schroeder, "Exploring hematopoiesis at single cell resolution.," *Cells Tissues Organs*, vol. 188, no. 1-2, pp. 139–149, 2008.

[3] Michael A Rieger, Philipp S Hoppe, Benjamin M Smejkal, Andrea C Eitelhuber, and Timm Schroeder, "Hematopoietic cytokines can instruct lineage choice.," *Science*, vol. 325, no. 5937, pp. 217–218, Jul 2009.

[4] Michael B Elowitz, Arnold J Levine, Eric D Siggia, and Peter S Swain, "Stochastic gene expression in a single cell.," *Science*, vol. 297, no. 5584, pp. 1183–1186, Aug 2002.

[5] Ariel A. Cohen, Naama Geva-Zatorsky, Eran Eden, Milana Frenkel-Morgenstern, Iirina Issaeva, Alex Sigal, Ron Milo, Cellina Cohen-Saidon, Yuvalal Liron, Zvi Kam, Lydia Cohen, Tamar Danon, Natalie Perzov, and Uri Alon, "Dynamic proteomics of individual cancer cells in response to a drug.," *Science*, vol. 322, no. 5907, pp. 1511–1516, Dec 2008.

[6] Andrew R Cohen, Francisco L A F Gomes, Badrinath Roysam, and Michel Cayouette, "Computational prediction of neural progenitor cell fates.," *Nat Methods*, vol. 7, no. 3, pp. 213–218, Mar 2010.

[7] Beate Neumann, Thomas Walter, Jean-Karim Hrich, Jutta Bulkescher, Holger Erfle, Christian Conrad, Phill Rogers, Ina Poser, Michael Held, Urban Liebel, Cihan Cetin, Frank Sieckmann, Gregoire Pau, Rolf Kabbe, Annelie Wnsche, Venkata Satagopam, Michael H A Schmitz, Catherine Chapuis, Daniel W Gerlich, Reinhard Schneider, Roland Eils, Wolfgang Huber, Jan-Michael Peters, Anthony A Hyman, Richard Durbin, Rainer Pepperkok, and Jan Ellenberg, "Phenotypic profiling of the human genome by time-lapse microscopy reveals cell division genes.," *Nature*, vol. 464, no. 7289, pp. 721–727, Apr 2010.

[8] Timm Schroeder, "Long-term single-cell imaging of mammalian stem cells.," *Nat Methods*, vol. 8, no. 4 Suppl, pp. S30–S35, Apr 2011.

[9] Timm Schroeder, "Imaging stem-cell-driven regeneration in mammals.," *Nature*, vol. 453, no. 7193, pp. 345–351, May 2008.

[10] Martin Ester, HansPeter Kriegel, Jörg Sander, and Xiaowei Xu, "A density-based algorithm for discovering clusters in large spatial databases with noise," 1996, pp. 226–231, AAAI Press.

[11] Michał Komorowski, Bärbel Finkenstädt, and David Rand, "Using a single fluorescent reporter gene to infer half-life of extrinsic noise and other parameters of gene expression.," *Biophys J*, vol. 98, no. 12, pp. 2759–2769, Jun 2010.

[12] Yuichi Taniguchi, Paul J Choi, Gene-Wei Li, Huiyi Chen, Mohan Babu, Jeremy Hearn, Andrew Emili, and X. Sunney Xie, "Quantifying e. coli proteome and transcriptome with single-molecule sensitivity in single cells.," *Science*, vol. 329, no. 5991, pp. 533–538, Jul 2010.

[13] Hanna M Eilken, Shin-Ichi Nishikawa, and Timm Schroeder, "Continuous single-cell imaging of blood generation from haemogenic endothelium.," *Nature*, vol. 457, no. 7231, pp. 896–900, Feb 2009.

[14] Christoph Sommer, Christoph Straehle, Ullrich Koethe, and Fred A. Hamprecht, "ilastik: Interactive learning and segmentation toolkit," in *8th IEEE International Symposium on Biomedical Imaging (ISBI 2011)*, 2011.

[15] Jae S. Lim, *Two-Dimensional Signal and Image Processing*, Englewood Cliffs, NJ, Prentice Hall, 1990.

[16] Joakim Lindblad and Ewert Bengtsson, "A comparison of methods for estimation of intensity nonuniformities in 2d and 3d microscope images of fluorescence stained cell," in *12th Scandinavian Conference on Image Analysis (SCIA)*, 2001.

[17] Alex Sigal, Ron Milo, Ariel Cohen, Naama Geva-Zatorsky, Yael Klein, Inbal Alaluf, Naamah Swerdlin, Natalie Perzov, Tamar Danon, Yuvalal Liron, Tal Raveh, Anne E Carpenter, Galit Lahav, and Uri Alon, "Dynamic proteomics in individual human cells uncovers widespread cell-cycle dependence of nuclear proteins.," *Nat Methods*, vol. 3, no. 7, pp. 525–531, Jul 2006.